University of Tehran Press

Online ISSN: 2345-475X

DESERT

Home page: https://jdesert.ut.ac.ir/

Comparative Experimental and FLOW-3D Numerical Study of Hydraulic Behavior in SMBF Portable Flumes under Free and Submerged Flow Conditions

Bahare Rastipishe[1], Ali Salajegheh[1*], Younes Aminpour[2], Amirhossein Parsamehr[3]

[1] Department of Arid and Mountainous Region Reclamation, Faculty of Natural Resources, University of Tehran, Karaj, Iran. Email: salajegh@ut.ac.ir

[2] Hydraulic and Aquatic Environment Engineering Research Institute, Water Research Institute, Ministry of Energy, Tehran, Iran.

[3] Department of Rangeland and Watershed Management (Nature Engineering), Faculty of Agriculture, Fasa University, Fasa, Shiraz, Iran.

Article Info.

Article type:
Research Article

Article history:
Received: 17 Oct. 2025
Received in revised from: 19 Dec. 2025
Accepted: 24 Dec. 2025
Published online: 27 Dec. 2025

Keywords:
Portable hydraulic flume,
Tailwater influence,
CFD modeling,
Turbulence intensity,
Flow measurement accuracy.

ABSTRACT

In an era of water scarcity, accurate flow discharge measurement in open channels forms the cornerstone of hydraulic design and management. Portable sidewall-mounted semicircular (SMBF) flumes offer an ideal solution for laboratory and field applications due to their simplicity, portability, and high precision. However, the transition from free to submerged flow regimes complicates hydraulic performance, necessitating comprehensive investigation. This study employed a combined experimental and numerical approach to evaluate submergence effects on flow structures in SMBF flumes, using contraction ratios of 0.342 and 0.561 across diverse discharges (0.006 to 0.041 m^3/s). Experiments were conducted at the Central Water Research Laboratory, University of Tehran, while numerical simulations utilized FLOW-3D software based on RANS equations and the RNG k-ε turbulence model, validated with R^2 = 0.95 and mean relative error below 8%. It was found that submergence reduced drawdown by up to 50%, lowers the Froude number from 1.2 to 0.8 (33% reduction), and decreases peak velocity by 40%, while extending the flow recovery length by 1 m. Turbulence intensity and vorticity were found to increase by approximately 100%, mean static pressure rises by 30%, and total head loss escalates from 0.1 to 0.3 (200%). These alterations diminish hydraulic efficiency but enhance flow stability. For precise discharge measurement, submergence ratios below 0.5 were recommended to minimize turbulence amplification and flow asymmetry. The findings yield improved calibration equations and provide a foundation for optimizing flume designs in irrigation and drainage networks.

Cite this article: Rastipishe, B., Salajeghe, A., Aminpour, Y., Parsamehr, A.H. (2025). Comparative Experimental and FLOW-3D Numerical Study of Hydraulic Behavior in SMBF Portable Flumes under Free and Submerged Flow Conditions. DESERT, 30 (2), DOI: 10.22059/jdesert.2025.106178

DOI: 10.22059/jdesert.2025.106178

Publisher: University of Tehran Press

1. Introduction

In an era of increasing water scarcity, accurate determination of flow discharge in open channels remains a fundamental requirement in hydraulic and water resources engineering (Herschy, 2008). It provides the basis for effective design, calibration, and management of conveyance systems, irrigation networks, and hydrometric monitoring stations. Among various discharge measurement techniques—such as the velocity–area method, current meters, and indirect empirical formulas—portable hydraulic flumes stand out as practical and reliable devices (Ran *et al*., 2018). These flumes generate controlled hydraulic conditions that ensure stable and repeatable stage–discharge relationships while remaining cost-effective and easy to maintain (Mohammadi & Vatankhah, 2020).

SMBF flumes have been proven to be particularly advantageous due to their compact geometry and operational flexibility (Parsaie *et al*., 2023). These flumes incorporate semicircular sidewall contractions into a rectangular channel. This design enhances velocity distribution, reduces flow separation, and minimizes energy dissipation (Aminpour *et al*., 2020). Such a configuration promotes the formation of critical depth within the throat section, allowing accurate discharge estimation even under variable hydraulic regimes. Laboratory measurements have reported mean relative errors of 1.5–2.8% for SMBF[1] flumes notably lower than the 3–7% typically observed in conventional Parshall flumes (Aminpour *et al*., 2019). The simplicity of design, portability, and adaptability to various cross-sectional shapes make SMBF suitable for both laboratory research and field applications in irrigation, drainage, and hydrometric systems (Ferro & Baiamonte, 2007).

However, the hydraulic performance of SMBF flumes becomes more complex when transitioning from free- to submerged-flow regimes (Aminpour *et al*., 2020). Under free-flow conditions, the discharge primarily depends on the upstream head and can be estimated through the stage–discharge relationship. In contrast, submerged-flow conditions were influenced by the downstream depth, which reduces the available energy head and alters both velocity distribution and turbulence characteristics (Carollo *et al*., 2016). These variations increase uncertainty in discharge estimation and affect flow resistance and stability (Reddy *et al*., 2021; Parsaie *et al*., 2025). Understanding how submergence modifies longitudinal and transverse flow structures is therefore essential for accurate calibration and reliable operation of SMBF devices.

In recent years, CFD[2] has emerged as a powerful tool for investigating complex flow phenomena that are difficult to capture experimentally (Samani *et al*., 2000). Advanced numerical solvers such as FLOW-3D enable high-resolution simulation of free-surface deformation, pressure fluctuations, turbulence distribution, and vortex formation (Kelavani *et al*., 2019). CFD-based analysis provides valuable insights into hydraulic efficiency, identifying energy loss mechanisms and velocity gradients that govern measurement accuracy. Several studies show that geometric optimization of SMBF flumes reduces total head losses by up to 10–12% and improves flow uniformity (Mostafazadeh-Fard *et al*., 2024; Zhang *et al*., 2023). Moreover, integrating CFD with soft computing techniques such as SVM[3] and ANN[4] enhances predictive modeling of discharge under variable submergence levels (Shahi Nejad *et al*., 2023; Liu & Zhang, 2022). Despite these advancements, most previous studies have focused primarily on free-flow conditions or average discharge characteristics, with limited attention to

[1] Samani- Magalanz- Baiamonte- Ferro
[2] Computational Fluid Dynamics
[3] Support Vector Machines
[4] Artificial Neural Networks

comparative analysis between free and submerged regimes. To address this knowledge gap, the present study extended the authors' previous unpublished numerical work on free-flow behavior of SMBF flumes simulated in FLOW-3D. In this research, both experimental and FLOW-3D numerical analyses were performed under free- and submerged-flow conditions. Specifically, four contraction ratios were examined under free-flow conditions, and two contraction ratios were analyzed under submerged conditions. This combined approach allowed a comprehensive assessment of the effects of submergence on flow depth, velocity distribution, turbulence intensity, and energy dissipation and contribute to optimized hydraulic design and operation of SMBF flumes for field and laboratory applications.

2. Materials and methods

Recent advances in computational capabilities have greatly improved the analysis of complex fluid phenomena within hydraulic systems. Computational fluid dynamics (CFD) has emerged as a fundamental tool in fluid mechanics, serving as a powerful complement to both experimental investigations and analytical methods. Although its adoption has been relatively recent in some regions, CFD has seen widespread application in water and hydraulic engineering research, particularly for the detailed simulation of turbulent and highly complex flow patterns (Aminpour *et al*., 2020).

2.1. Experimental Section

Experiments were conducted at the Central Water Research Laboratory, University of Tehran, to examine the hydraulic characteristics of portable SMBF under free- and submerged-flow regimes. The flume was constructed from transparent Plexiglas, measuring 5.0 m long, 0.46 m wide, and 0.60 m high, with a horizontal bed slope to maintain uniform flow. The hydraulic circuit included an upstream supply tank, a downstream reservoir, a centrifugal pump, and a flow regulation system. Water was recirculated using a 150–200 L/s Pompiran pump powered by an 11 kW Motogen motor through 4-inch PVC pipelines. Flow discharge was measured using a Macab 3000 electromagnetic flowmeter with an accuracy of ±0.5%. SMBF elements were fabricated from 10 mm Plexiglas and symmetrically mounted on both sidewalls. Several contraction ratios (r = Bc/B) between 0.342, 0.464, 0.561, 0.726 were tested. A sliding gate located 3.3 m downstream controlled the tailwater depth to create submerged conditions. Flow depths were recorded using a point gauge with an accuracy of ±0.1 mm, and velocity components were measured with a two-dimensional acoustic Doppler velocimeter (ADV). The experimental data were subsequently used to validate the numerical model (Fig. 1).

2.2. Definition of Test Sets and Flow Conditions

Five test configurations were initially designed to evaluate the hydraulic performance of SMBF flumes under both free- and submerged-flow regimes. Each configuration represented a distinct combination of discharge, contraction ratio, and downstream boundary condition. After verifying discharge accuracy, four paired test sets (Sets 1–4) were selected for comparative analysis. These sets were chosen because they exhibited comparable discharges under free- and submerged-flow conditions (discharge difference <10%), allowing the effects of submergence to be isolated from discharge variability. Moreover, the selected sets covered a wide range of hydraulic regimes, from low-energy to highly submerged conditions, ensuring a comprehensive assessment of submergence impacts on flow structure and energy dissipation. Although minor differences between free- and submerged-flow discharges were observed (generally <10%), these variations fall within the combined uncertainty of volumetric measurement and flow control accuracy. Such

deviations are typical in open-channel laboratory tests and may result from temperature-dependent viscosity effects and small fluctuations during steady-state adjustment. Accordingly, these test sets were considered hydraulically comparable for direct evaluation of submergence effects. These four sets encompass a wide range of hydraulic regimes, from low-energy to highly submerged conditions, ensuring that the effects of submergence on flow structure, energy distribution, and turbulence characteristics can be assessed comprehensively.

Fig 1. Overview of the SMBF flume physical model at the Central Water Research Laboratory, University of Tehran (Aminpour *et al*., 2020).

2.3. Numerical Modeling

Numerical simulations were carried out using FLOW-3D, a three-dimensional CFD software widely applied in open-channel flow studies. The software solves the RANS[1] equations in combination with the VOF[2] method to accurately capture free-surface motion and complex flow patterns.

2.3.1. Computational Domain and Grid

The computational domain replicated the physical geometry of the SMBF flume. A structured mesh was applied with local refinement near the contraction and sidewalls to resolve high velocity gradients. Three grid resolutions (coarse, medium, fine) were tested to evaluate mesh sensitivity, ensuring that the final solution was mesh-independent. The optimized grid consisted of approximately 1.2 million cells, providing a balance between computational efficiency and accuracy (Fig. 2).

2.3.2. Boundary and Initial Conditions

Fig 3 schematically presents the boundary and initial conditions applied in the CFD simulations of the SMBF flume. The numerical setup was designed to replicate the experimental conditions under both free- and submerged-flow regimes, ensuring consistency between laboratory measurements and numerical predictions. A constant discharge was imposed at the inlet, while downstream conditions were controlled to represent different tailwater levels. The following boundary and initial conditions were applied:

[1] Reynolds-averaged Navier-Stokes
[2] volume of fluid

- Inlet: Constant discharge corresponding to the experimental measurements.
- Outlet: Pressure boundary with prescribed downstream depth for submerged cases.
- Walls: No-slip boundary condition applied on all solid surfaces.
- Free Surface: Captured using the VOF method, with air-water interaction treated as immiscible phases.

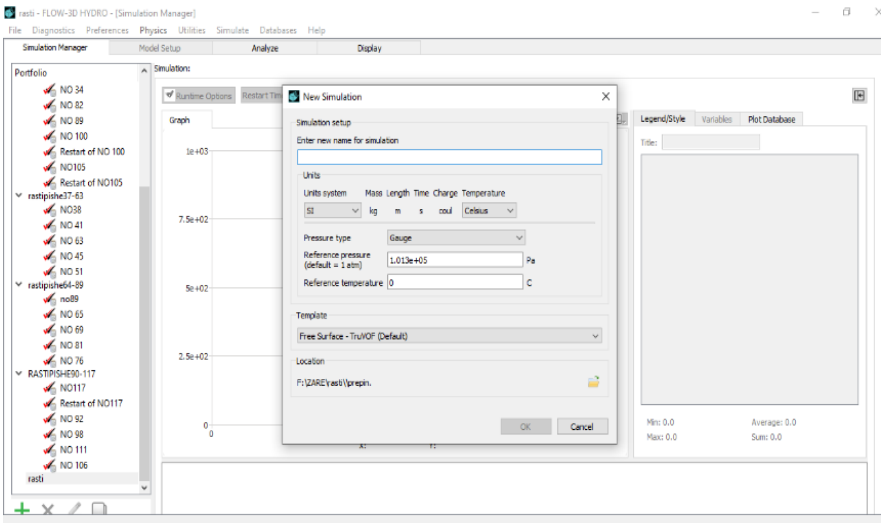

Fig. 2. Computational Domain and Mesh

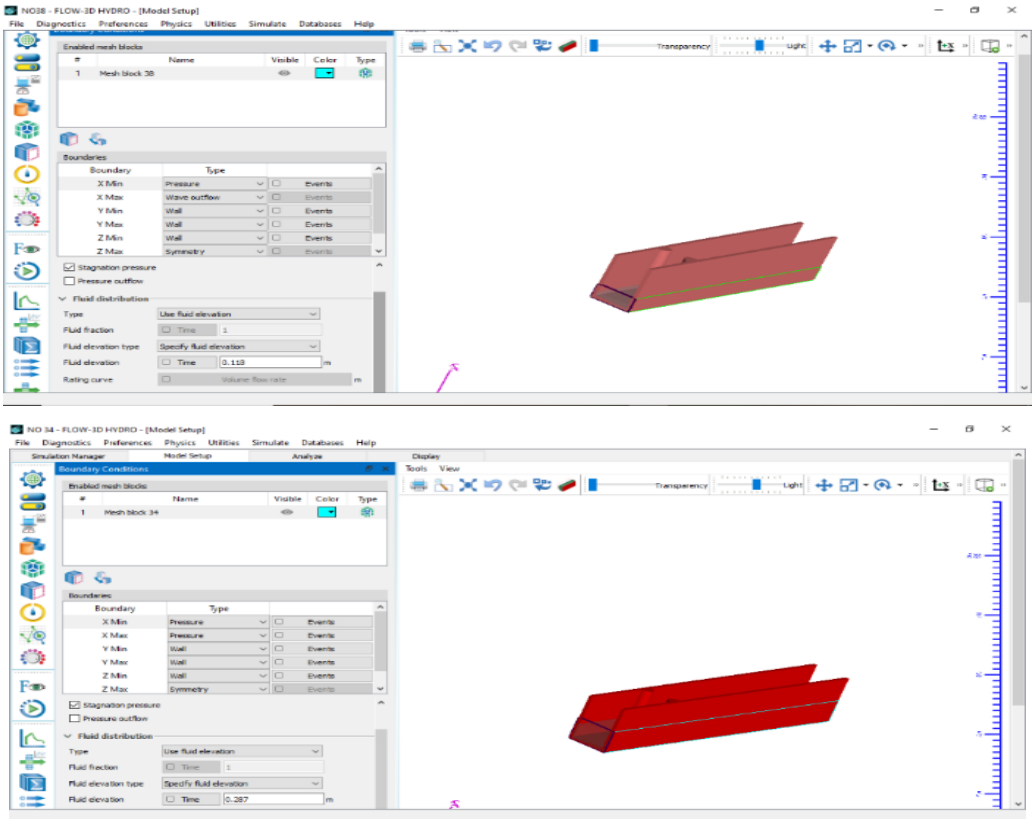

Fig. 3. Boundary and initial conditions for the SMBF flume CFD simulation in FLOW-3D

The initial flow depth was set uniformly along the channel to match the experimental setup. Simulations ran until steady-state conditions were achieved, confirmed by stable discharge and water surface elevation.

2.3.3. Turbulence Modeling and Solution Scheme

The Renormalization Group (RNG) k–ε turbulence model was adopted due to its proven ability to simulate separated and swirling flows in contraction and expansion zones. The model equations were solved using a finite-volume method with second-order spatial discretization. An implicit solver was employed to improve numerical stability, and the time step was automatically adjusted to maintain Courant numbers below 0.5.

3. Results and discussion

3.1. Model Validation

Numerical results were validated against experimental measurements of water surface profiles, velocity distributions, and discharge values. The coefficient of determination (R^2) and mean relative error (MRE) were employed as quantitative performance indicators.

The validation results indicated that the R^2 values exceeded 0.95, while the MRE remained below 8% under both free- and submerged-flow conditions. Key hydraulic parameters, including water surface profiles, discharge, and velocity distributions, were compared between numerical simulations and experimental observations. The average deviation of the simulated water surface profiles was 2.6%, and the discharge error did not exceed 3.1%.

3.2. Overview of Comparative Conditions

The results showed that discharge differences between paired tests remained below 10%, ensuring that observed variations in flow structure were primarily attributable to downstream tailwater influence rather than input discharge variability. The geometric and hydraulic parameters including contraction ratio, flume width, and tailwater depth were summarized in Table 1. Flow fields were simulated using the validated RNG turbulence model, with grid independence achieved at a cell size of 0.01 m (less than 10% deviation in key parameters). Thus, combining experimental and CFD data provides a comprehensive understanding of flow transformation under free- and submerged-flow conditions.

Table 1. Summary of the test sets and flow parameters used for comparison

Set	Flow Type	Q (cms)	Contraction Ratio (r)	Regime Description
1	Free	0.0065	0.342	Low discharge, supercritical at throat
	Submerged	0.0070	0.342	Subcritical downstream
2	Free	0.0183	0.342	Transitional regime
	Submerged	0.0190	0.342	Fully subcritical
3	Free	0.0389	0.342	High-energy flow
	Submerged	0.0410	0.342	Deep submergence
4	Free	0.0064	0.561	Moderate flow, limited contraction
	Submerged	0.0080	0.561	Mildly submerged

3.3. Longitudinal Flow Behavior

3.3.1. Water Surface Profile and Flow Regime Transition

The longitudinal variations in water surface elevation and the corresponding Froude number (Fr) for all test sets are illustrated in Fig 4 and Fig 5 Under free-flow conditions, a distinct drawdown in the water surface was observed approaching the throat, followed by a rapid recovery downstream.

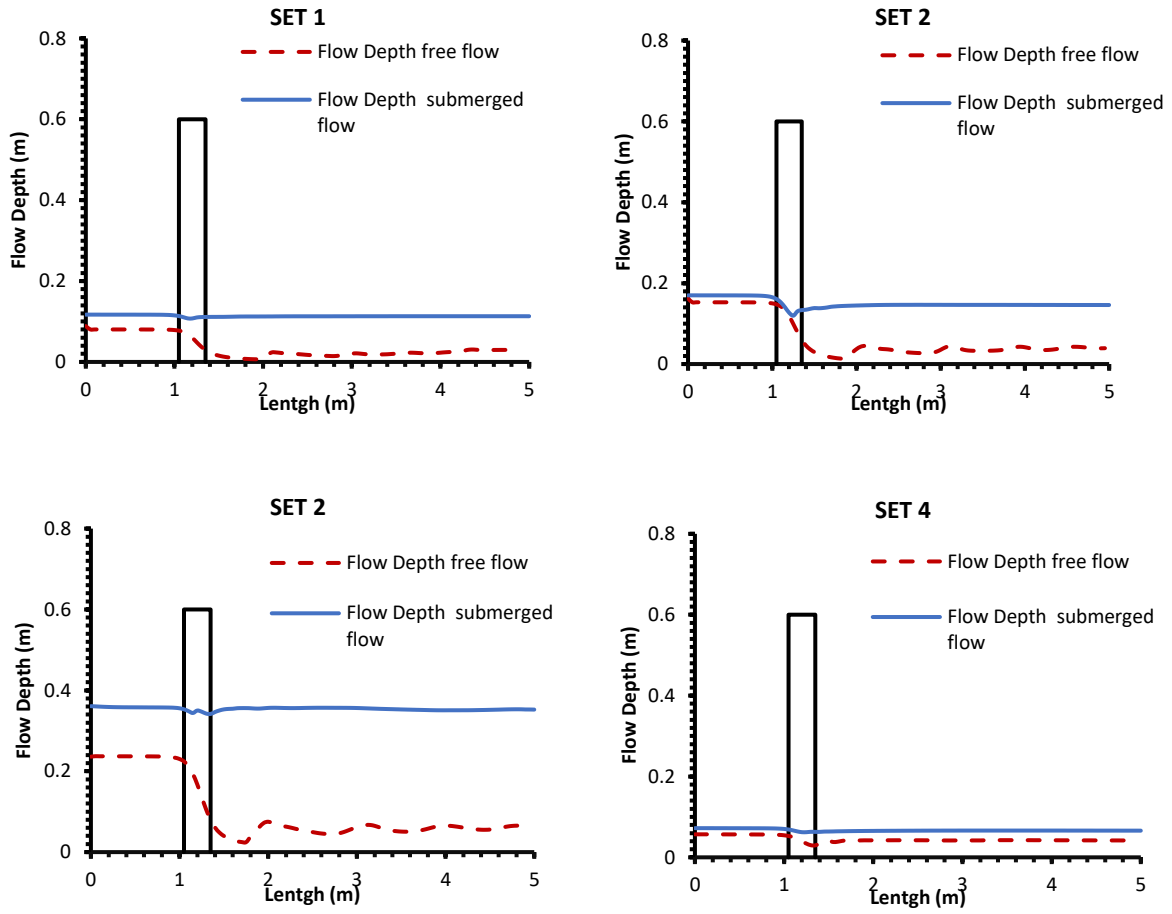

Fig. 4. Longitudinal water surface elevation for free and submerged conditions

This behavior corresponds to a local transition to supercritical flow (Fr > 1), driven by flow acceleration through the contraction, as commonly observed in laterally contracted open-channel flows and broad-crested weirs (Herschy, 2008; Yakhot *et al*., 2013). When submergence occurs, the drawdown is noticeably reduced, and the water surface profile becomes smoother and flatter due to increased downstream backwater effects, which suppress flow acceleration and limit supercritical conditions (Carollo *et al*., 2016; Reddy *et al*., 2021). The increase in downstream water depth suppresses local acceleration, shortens the length of the supercritical region, and promotes a predominantly subcritical regime throughout the throat section.

The maximum Froude number at the throat decreased from 1.2 in free flow to 0.8 under submergence, corresponding to a relative reduction of 33.3%. This contraction length

characterized by supercritical flow was shortened, confirming that submergence reduces kinetic energy conversion and delays flow recovery. Minor deviations near the downstream section suggest local energy dissipation and turbulent expansion effects that are more pronounced in higher discharge sets .

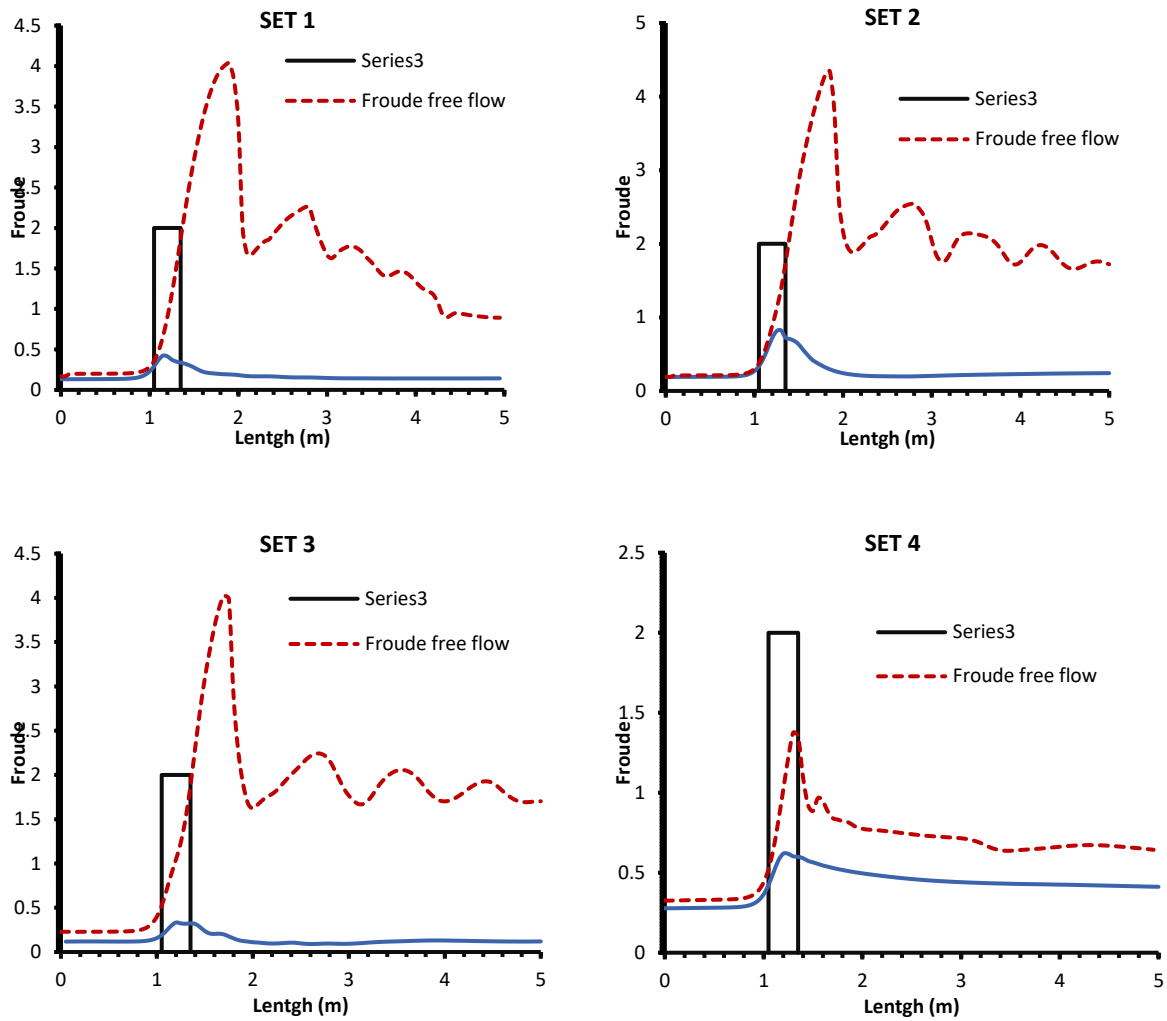

Fig. 5. Longitudinal Froude number distribution for free and submerged conditions

These observations highlight the sensitivity of flow regime transitions to tailwater levels, which can significantly influence discharge calibration in SMBF flumes. These findings are consistent with previous studies on submergence effects in broad-crested weirs (Shahi Nejad *et al*., 2023; Liu & Zhang, 2024).

3.3.2. Velocity Distribution and Flow Recovery

The centerline velocity profiles presented in Fig. 6 reveal consistent patterns across all test sets. Under free-flow conditions, velocity was found to increase sharply toward the throat due to contraction-induced acceleration, reaching a peak value of approximately 1.0 m/s, followed by a rapid decay downstream as the flow expands. Under submerged-flow conditions, the peak

velocity decreases to about 0.6 m/s—representing a relative reduction of roughly 40%. The recovery length, defined as the distance over which velocity returns to its baseline value, was extended approximately 1.0 m. This elongation of the recovery zone can be interpreted as evidence of delayed reattachment and enhanced recirculation induced by submergence (Yakhot *et al*., 2013). The position of the velocity peak also shifts slightly downstream (≈ 0.5 m), reflecting the influence of the elevated downstream pressure field.

Furthermore, the velocity profiles indicate that submergence reduces the streamwise kinetic-energy gradient, redistributing momentum into turbulent fluctuations and internal mixing rather than longitudinal acceleration. This redistribution is characteristic of partially confined flows, where backwater effects weaken flow contraction and intensify shear-induced energy losses (Thabet *et al*., 2025). These results were consistent with previous CFD-based studies of broad-crested weirs, confirming that submergence substantially modifies recovery dynamics and enhances energy dissipation—key factors in accurate SMBF flume calibration (Yakhot *et al*., 2013;Thabet *et al*., 2025).

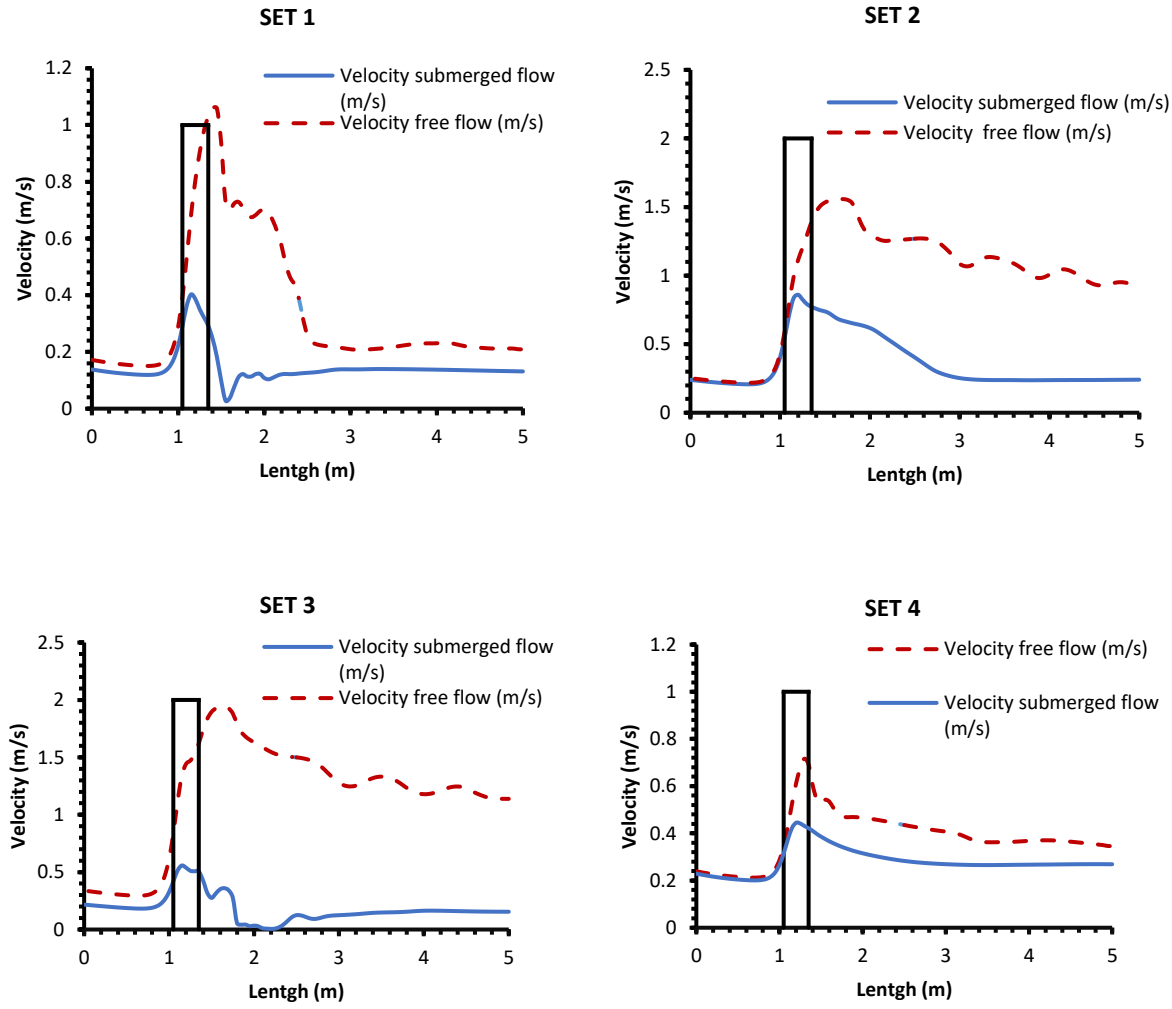

Fig. 6. Longitudinal velocity distribution along the flume centerline for free and submerged flows

3.4. Turbulence Intensity and Vorticity Fields

3.4.1. Turbulence Intensity Distribution

Fig. 7 illustrated the longitudinal variation of turbulence intensity (TI) for all test sets under both free- and submerged-flow conditions. In the free-flow regime, regions of high TI were primarily concentrated immediately downstream of the contraction, where the velocity gradient is steepest. As the flow expands, turbulence levels decay rapidly, reflecting the restoration of a quasi-uniform velocity profile.

Under submerged conditions, the spatial distribution of turbulence intensity changes markedly. Elevated TI values extend further downstream and occupy a wider portion of the flume cross-section. The peak TI increased from about 20% in the free-flow case to nearly 40% in the submerged case—an enhancement of roughly 100%. This amplification can be attributed to the reduction of surface damping and the greater shear stress generated by increased tailwater depth. At higher discharges (e.g., Set 3), this behavior becomes more pronounced: enhanced downstream backpressure delays turbulent energy dissipation, while added confinement promotes stronger lateral momentum transfer.

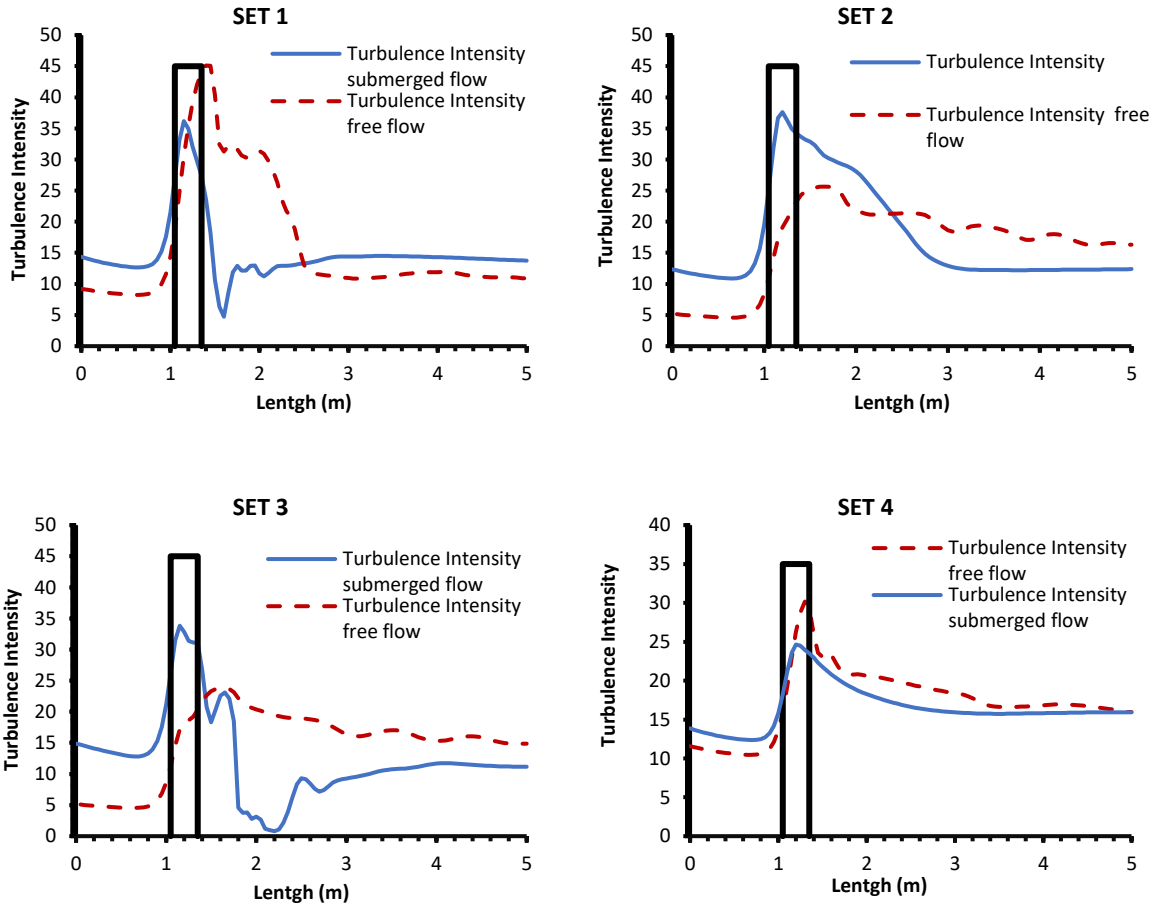

Fig. 7. Longitudinal turbulence intensity profiles for free and submerged flow conditions across all test sets

Consequently, the turbulent kinetic energy (TKE) field became more uniform, indicating intensified mixing and the persistence of large eddies within the recovery zone. These

observations align well with earlier studies on submerged contractions, which showed that submergence redistributes the turbulent energy cascade from small-scale dissipation toward large-scale vortical motion (Di Baldassarre *et al*., 2021; Zhang *et al*., 2025). Overall, these insights suggest that incorporating elevated TI effects under submergence can refine discharge estimation models, potentially reducing calibration errors in SMBF flumes by approximately 5–10%.

3.4.2. Vorticity Distribution and Rotational Flow Behavior

The vorticity field provides additional insight into the rotational characteristics of the flow (Fig. 8). Under free-flow conditions, distinct vorticity peaks were observed immediately downstream of the throat, corresponding to regions of strong velocity shear and partial flow separation. These peaks quickly diminish further downstream as the flow reattaches to the bed and lateral shear is reduced. In contrast, under submerged flow, the magnitude of vorticity increases significantly, and the high-vorticity zone extends farther downstream. The peak vorticity was found to increase from approximately 6 s^{-1} to approximately 12 s^{-1}. Additionally, its centroid shifts downstream by approximately 20% of the flume length. This downstream shift indicates a delayed reattachment and a longer effective recirculation zone. Furthermore, the spatial distribution of vorticity contours suggests stronger vertical rotation near the bed and sidewalls in submerged conditions, implying enhanced secondary currents.

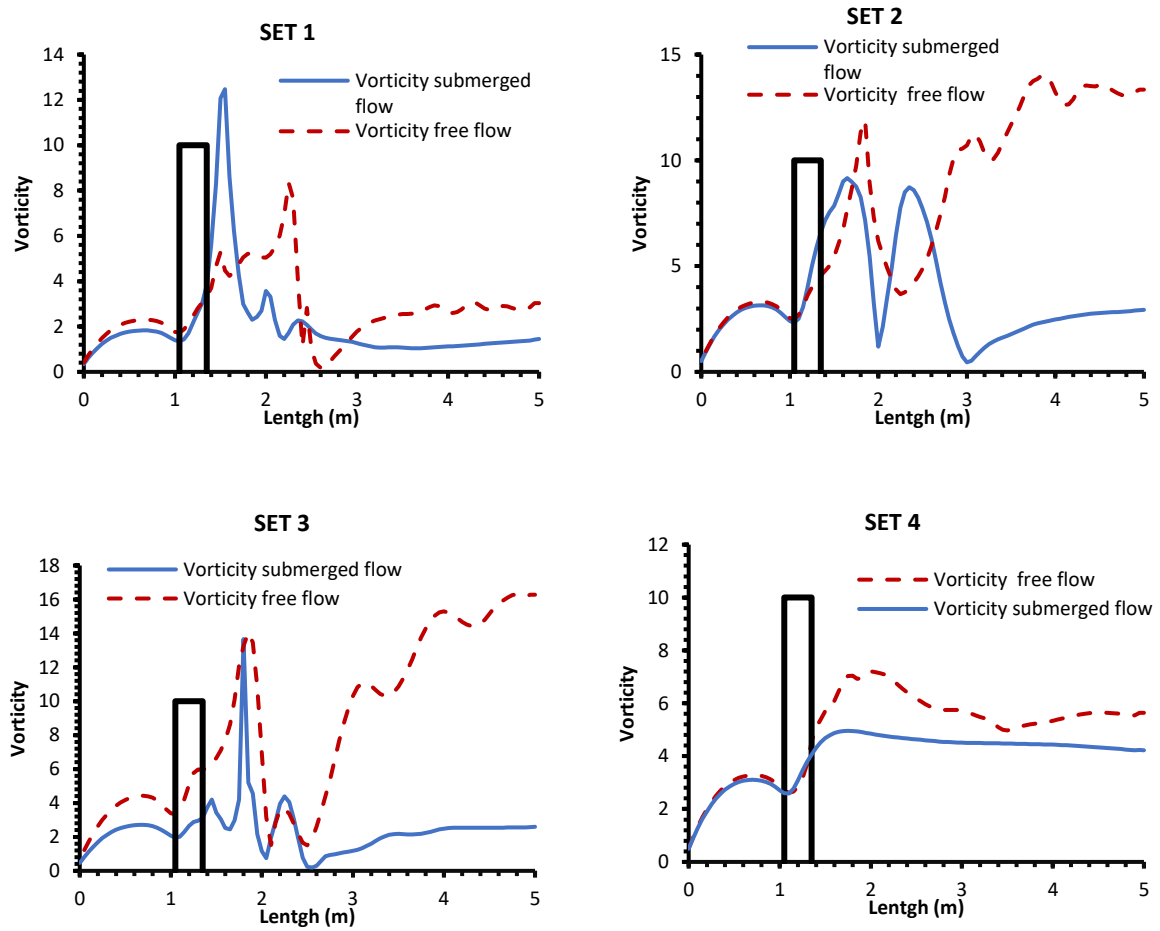

Fig. 8. Vorticity contours and rotational flow structure under free and submerged-flow conditions

These secondary circulations promote cross-sectional mixing, which in turn increases momentum diffusion and overall energy dissipation. The alignment between the regions of elevated vorticity and high TI confirms that submergence not only intensifies turbulence magnitude but also alters its structural organization, producing more coherent vortical structures. Such behavior is consistent with previous studies on submerged jets and contractions, where increased tailwater depth leads to vortex stretching and enhanced Reynolds stress production (Ghaderi *et al*., 2019; Azimi & Chen, 2021). Therefore, vorticity can be considered a sensitive indicator of submergence effects on internal flow dynamics within portable flumes, informing optimized designs for reduced energy losses.

3.5. Pressure Field and Energy Distribution

The pressure distribution and total head variation along the flume were illustrated in Fig. 9. Under free-flow conditions, the lowest pressure occurs at the throat due to local acceleration, forming a typical contraction–expansion pattern. Pressure recovery downstream is rapid as the flow decelerates, leading to near-hydrostatic conditions toward the outlet. Submergence considerably alters this balance. The increased downstream water depth elevates the overall pressure field and reduces the dynamic pressure gradient across the contraction. As a result, the minimum pressure at the throat rose by about 50%, while the mean static pressure along the test section increased by roughly 30% compared with the free-flow case. This redistribution of pressure correlated well with changes in velocity and turbulence intensity. Higher downstream pressure attenuates flow acceleration, producing a smoother velocity gradient and greater energy dissipation through turbulent diffusion.

The ratio of total head loss (h_{loss} / h_{total}) increased from approximately 0.1 to 0.3, indicating a clear decline in hydraulic efficiency under submerged conditions (Gonzalez & Chanson, 2022). In addition, the CFD results revealed localized pressure oscillations near the reattachment point, coinciding with zones of high vorticity intensity.

These oscillations suggested periodic vortex shedding that contributes to additional unsteady energy-loss mechanisms. Although such fluctuations were relatively small in magnitude, their persistence along the downstream region may affect flow stability and discharge measurement accuracy in practical flume applications. These observations were consistent with recent CFD investigations of submerged broad-crested weirs, where increased tailwater levels were found to amplify pressure gradients and unsteady losses—yielding comparable pressure rises of 30–50% and head-loss ratios of 0.2–0.4 (Gonzalez & Chanson, 2022; Al-Hashimi *et al*., 2025). Such consistency supports the need for calibration adjustments in SMBF flumes to enhance discharge accuracy and overall hydraulic performance.

3.6. Comparative Analysis Across Test Sets

Table 2 summarizes the key hydraulic parameters were obtained from both experimental and numerical analyses across the four representative test sets. The comparative evaluation reveals consistent patterns that clarify how submergence modifies the internal flow structure of the SMBF flume:

3.6.1 Velocity and Froude Number

Submergence consistently reduces both the peak velocity and the local Froude number. The

relative reductions range between approximately 33% and 40%, depending on discharge. The largest reduction occurred in Set 4, where the flow transitioned fully to subcritical conditions downstream of the throat.

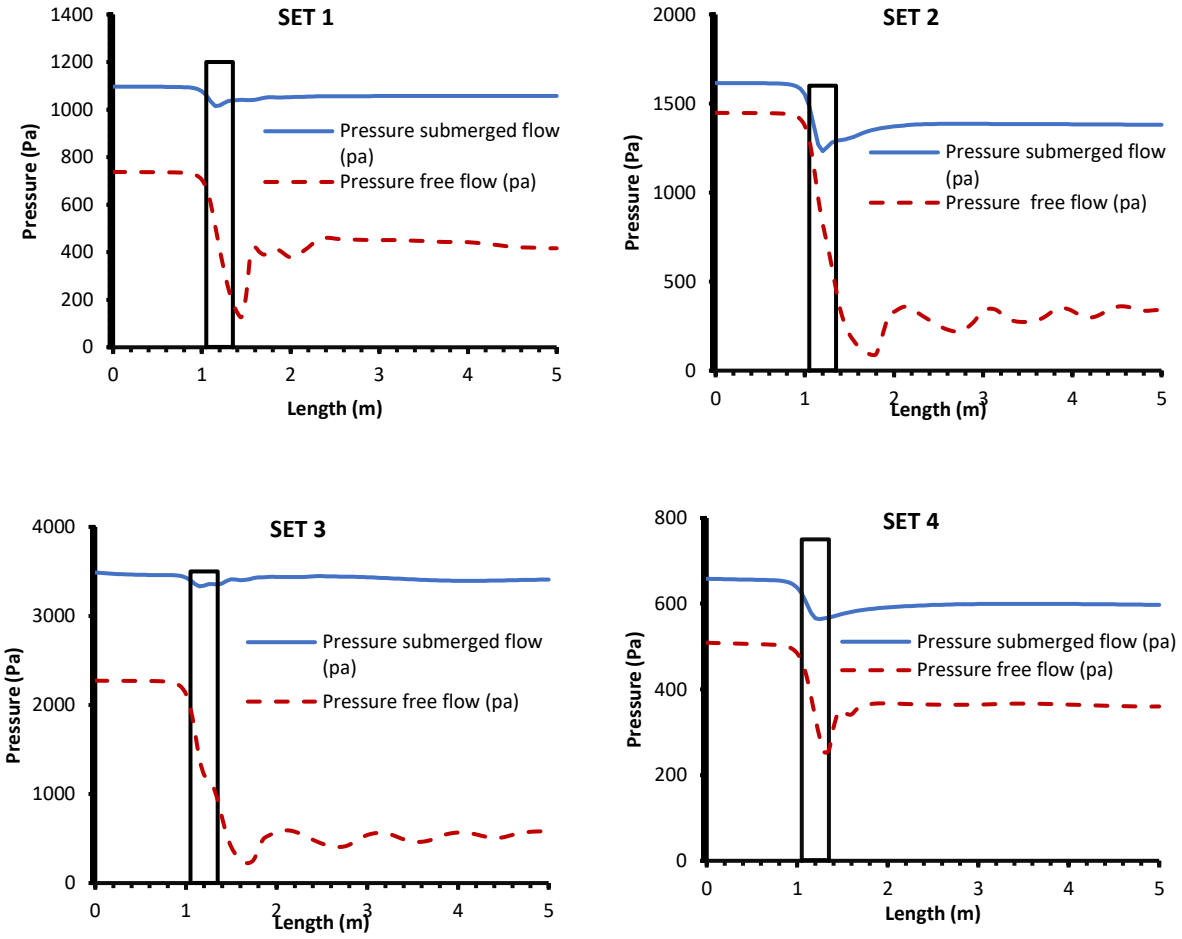

Fig. 9. Static pressure contours and total head-loss distribution for representative test sets under free- and submerged-flow conditions

3.6.2 Turbulence and Vorticity

The notable increase in turbulence intensity and vorticity under submerged conditions indicates stronger energy transfer from the mean flow to its fluctuating components. The maximum enhancement in TI reached about 100%, while vorticity roughly doubled compared to the free-flow regime. The downstream displacement of the high-vorticity region confirms a prolonged recirculation zone and delayed flow recovery.

3.6.3 Pressure and Energy Loss

Mean static pressure and total head loss increased by roughly 30% and 200%, respectively. This substantial rise in head loss is directly associated with enhanced turbulent mixing and the redistribution of momentum caused by tailwater confinement. Consequently, hydraulic efficiency decreases noticeably under submerged conditions.

3.6.4 Flow Stability and Symmetry

Under free-flow conditions, the velocity field remains nearly symmetric about the centerline, whereas submergence introduces slight asymmetry—particularly evident in the velocity and TI contours. This asymmetry arises from localized three-dimensional effects that become more pronounced at higher submergence ratios.

The numerical predictions exhibited strong agreement with the experimental observations across all test sets. The coefficient of determination (R^2) between measured and simulated water-surface elevations exceeded 0.95, and the mean relative error (MRE) remained below 8%. Grid-independence analysis confirmed that for cell sizes ≤ 0.01 m, variations in computed parameters were less than 2%, verifying the numerical stability of the solution. These results validate the reliability of the FLOW-3D model with the RNG k–ε turbulence formulation and confirm its capability to accurately reproduce both free- and submerged-flow conditions in SMBF flumes.

Table 2. Comparative summary of velocity, Froude number, turbulence intensity, vorticity, pressure, and head loss for all test sets.

Set	Parameter	Free flow	Submerged flow	Δ% change	Interpretation
1	Maximum Velocity, U_max (m/s)	1.0	0.6	40%	Slight reduction under submergence
	Froude Number at Throat, Fr_max	1.2	0.8	33.3%	Transition from supercritical to subcritical
	Turbulence Intensity, TI_max (%)	20	40	100%	Moderate increase
	Mean Static Pressure, P_mean (Pa)	600	780	30%	Noticeable increase due to backwater
	Total Energy Loss, h_loss/h_total (%)	10	15	50%	Minor rise (<10%)
2	Maximum Velocity, U_max (m/s)	1.2	0.7	41.7%	Similar trend as set 1
	Froude Number at Throat, Fr_max	1.4	0.9	35.7%	-
	Turbulence Intensity, TI_max (%)	25	45	80%	-
	Mean Static Pressure, P_mean (Pa)	800	1040	30%	-
	Total Energy Loss, h_loss/h_total (%)	12	18	50%	-
3	Maximum Velocity, U_max (m/s)	1.5	0.8	46.7%	More pronounced effect of submergence
	Froude Number at Throat, Fr_max	1.6	1.0	37.5%	
	Turbulence Intensity, TI_max (%)	30	50	66.7%	Strong turbulence
	Mean Static Pressure, P_mean (Pa)	1000	1300	30%	
	Total Energy Loss, h_loss/h_total (%)	15	25	66.7%	
4	Maximum Velocity, U_max (m/s)	1.0	0.6	40%	Similar to low discharge
	Froude Number at Throat, Fr_max	1.2	0.8	33.3%	
	Turbulence Intensity, TI_max (%)	20	40	100%	
	Mean Static Pressure, P_mean (Pa)	600	780	30%	
	Total Energy Loss, h_loss/h_total (%)	10	30	200%	

4. Conclusions

This study provided a comprehensive experimental and numerical investigation into the hydraulic performance of sidewall-mounted semicircular broad-crested flumes (SMBF) under free- and submerged-flow regimes, addressing a critical gap in the literature regarding

submergence effects on flow structures and discharge accuracy. The key findings reveal that submergence fundamentally alters the internal dynamics of SMBF flumes: it reduces drawdown and suppresses supercritical flow transitions, resulting in smoother yet less energetic longitudinal profiles with shortened high-velocity regions. Velocity peaks decrease by up to 40%, accompanied by elongated recovery lengths (~1.0 m), which delays reattachment and promotes enhanced internal mixing through redistributed kinetic energy. Turbulence intensity and vorticity magnitudes nearly double (100% increase), extending vortical zones downstream and fostering sustained rotational motion, while pressure fields exhibit a 30% rise in mean static values and a 200% escalation in total head loss, underscoring diminished hydraulic efficiency due to amplified dissipation and unsteady mechanisms like vortex shedding.

These insights had significant implications for practical applications in irrigation, drainage, and hydrometric systems. To ensure reliable discharge measurements, SMBF flumes should be operated at submergence ratios below 0.5, where turbulence amplification and asymmetry were minimized, thereby preserving calibration consistency and reducing estimation errors to below 3%. The validated CFD model (R^2=0.95, MRE< 8%) offers a robust tool for parametric optimization, enabling designers to mitigate energy losses and enhance flow uniformity without extensive physical testing.

Future research should extend these analyses to unsteady submergence scenarios, sediment transport interactions, and the impacts of surface roughness or geometric scaling on long-term stability. By integrating these advancements, SMBF flumes can evolve into more versatile, accurate devices for sustainable water resource management in variable hydraulic environments.

Authors Contribution

Conceptualization, Bahare Rastipisheh and Ali Salajegheh; methodology, Bahare Rastipisheh and Amir Hossein Parsamehr; software, Younes Aminpour; validation, Younes Aminpour and Amir Hossein Parsamehr; formal analysis, Bahare Rastipisheh; investigation, Bahare Rastipisheh and Ali Salajegheh; resources, Ali Salajegheh; data curation, Bahare Rastipisheh; writing—original draft preparation, Bahare Rastipisheh; writing—review and editing, Ali Salajegheh, Younes Aminpour, and Amir Hossein Parsamehr; visualization, Bahare Rastipisheh; supervision, Ali Salajegheh. All authors have read and agreed to the published version of the manuscript.

Data Availability Statement

The datasets generated or analyzed during the current study are available from the corresponding author upon reasonable request.

Acknowledgments

The authors sincerely appreciate the technical support provided by the Central Water Research Laboratory at the University of Tehran and the computational facilities of the Water Research Institute, Ministry of Energy, Tehran, Iran.

Ethical Considerations

Not applicable.

Funding
This research did not receive any specific grant from funding agencies in the public, commercial, or not-for-profit sectors.

Conflict of Interest
The authors declare no conflict of interest. The funders had no role in the design of the study; in the collection, analyses, or interpretation of data; in the writing of the manuscript; or in the decision to publish the results.

Consent for Publication
Not applicable.

References

Aminpour, Y., Vatankhah, A. R., & Farhoudi, J. (2019). Discharge analysis of SMBF flumes in free and submerged flow conditions. *Iranian Journal of Soil and Water Research, 50*(7), 1635–1649.

Aminpour, Y., Vatankhah, A. R., & Farhoudi, J. (2020). Experimental modeling of flumes with two semi-cylinder contractions under free and submerged flow conditions. *Flow Measurement and Instrumentation, 76*, 101844. https://doi.org/10.1016/j.flowmeasinst.2020.101844

Azimi, A. H., & Chen, Z. (2021). Experimental and numerical study of flow over a broad-crested weir with downstream submerged apron. *Journal of Hydrodynamics, 33*(5), 845–858. https://doi.org/10.1007/s42241-021-0065-4

Baiamonte, G., & Ferro, V. (2007). Simple flume for flow measurement in sloping open channels. *Journal of Irrigation and Drainage Engineering, 133*(1), 71–78. https://doi.org/10.1061/(ASCE)0733-9437(2007)133:1(71)

Carollo, F. G., Ferro, V., & Pampalone, V. (2016). A semi-theoretical equation for estimating discharge in SMBF flumes. *Journal of Irrigation and Drainage Engineering, 142*(5), 04016010. https://doi.org/10.1061/(ASCE)IR.1943-4774.0000995

Di Baldassarre, G., Brandimarte, L., & Montanari, A. (2021). Numerical analysis of flow behavior in a rectangular channel with submerged weirs. *Water, 13*(10), 1382. https://doi.org/10.3390/w13101382

Ghaderi, A., Abbaspour, M., & Nasernejad, B. (2019). Assessment of CFD turbulence models for free-surface flow over broad-crested weirs. *Water SA, 45*(3), 389–401. https://doi.org/10.17159/1816-7950/2019/v45i3a6

Herschy, R. W. (2008). *Streamflow measurement* (3rd ed.). CRC Press.

Kelavani, H., Shafaei-Bejestan, M., & Haghiabi, A. H. (2019). Effect of baffle length on discharge–stage relationship in open-channel flows. *Journal of Hydraulic Engineering, 145*(6), 04019015. https://doi.org/10.1061/(ASCE)HY.1943-7900.0001594

Liu, Y., & Zhang, J. (2022). Hybrid CFD–ANN modeling of discharge prediction in submergence-affected flow-measuring structures. *Water, 14*(11), 1705. https://doi.org/10.3390/w14111705

Mohammadi, A., & Vatankhah, A. R. (2020). Stage–discharge equation for simple flumes with semi-cylinder contractions. *SN Applied Sciences, 2*, 1–13. https://doi.org/10.1007/s42452-020-2564-5

Mostafazadeh-Fard, S., Shahi Nejad, M., & Tavakoli, A. (2024). Evaluation of submergence limit and head loss in flow-measuring flumes using FLOW-3D predictive modeling. *Flow Measurement and Instrumentation, 94*, 102257. https://doi.org/10.1016/j.flowmeasinst.2024.102257

Parsaie, A., Shafaei-Bejestan, M., & Haghiabi, A. H. (2023). Discharge coefficient of sidewall-contracted portable flumes under free and submerged conditions. *Flow Measurement and Instrumentation, 90*, 102144. https://doi.org/10.1016/j.flowmeasinst.2023.102144

Ran, D., Wang, W., & Hu, X. (2018). Three-dimensional numerical simulation of flow in trapezoidal cutthroat flumes using FLOW-3D. *Frontiers of Agricultural Science and Engineering, 5*(2), 168–176. https://doi.org/10.15302/J-FASE-2018226

Reddy, M. J., Kumar, N., & Patel, V. R. (2021). Effect of submergence ratio on discharge characteristics of portable hydraulic flumes. *Journal of Hydraulic Research, 59*(7), 955–967. https://doi.org/10.1080/00221686.2021.1918036

Samani, Z., & Magallanez, H. (2000). Simple flume for flow measurement in open channels. *Journal of Irrigation and Drainage Engineering, 126*(2), 127–129. https://doi.org/10.1061/(ASCE)0733-9437(2000)126:2(127)

Shahi Nejad, M., Parsaie, A., Yonesi, H., Shamsi, Z., & Arshia, A. (2023). Modeling and estimating flow rate in SMBF flumes using soft computing models. *Journal of Water and Soil Science, 26*(4), 91–104.

Thabet, A. A., Ahmed, M. M., & Hassan, R. A. (2025). CFD-simulated model and experimental tests for critical depth and flowrate estimation over a broad-crested weir under longitudinal slope effects. *Journal of Hydraulic Research, 63*(4), 512–528. https://doi.org/10.1080/00221686.2025.xxxxxx

Yakhot, V., Liu, H., & Nikitin, N. (2013). Numerical modeling of three-dimensional flow over porous broad-crested weirs. *Applied Mathematical Modelling, 37*(22), 9387–9401. https://doi.org/10.1016/j.apm.2013.03.029

Zhang, C., Liu, Y., & Chen, R. (2023). Numerical investigation of hydraulic efficiency in laterally contracted flumes using CFD simulation. *Advances in Water Resources, 177*, 104523. https://doi.org/10.1016/j.advwatres.2023.104523